AJR FOCUS ON:

Neonatal Bowel Disorders: Practical Imaging Algorithm for Trainees and General Radiologists

Anh-Vu Ngo[1]
A. Luana Stanescu
Grace S. Phillips

OBJECTIVE. Neonatal bowel disorders require prompt and accurate diagnosis to avoid potential morbidity and mortality. Symptoms such as feeding intolerance, emesis, or failure to pass meconium may prompt a radiologic evaluation.

CONCLUSION. We discuss the most common neonatal bowel disorders and present a practical imaging algorithm for trainees and general radiologists.

Neonatal bowel disorders comprise a variety of congenital and acquired entities of both the upper and lower gastrointestinal (GI) tracts. We focus our discussion on the most common entities for which radiologic evaluation plays a substantial role in diagnosis. We first outline a general radiologic approach to these disorders and subsequently elaborate on individual diseases. Although some neonatal bowel disorders may be diagnosed prenatally, a discussion of prenatal features is largely beyond the scope of this article. With respect to the upper GI tract, we will describe esophageal atresia (EA) and tracheoesophageal fistula (TEF); pyloric stenosis; duodenal web, stenosis, and atresia; and malrotation. Regarding the lower gastrointestinal tract, we will discuss jejunoileal and colonic atresias, meconium ileus, anorectal malformations, functional immaturity of the colon, Hirschsprung disease (HD), and necrotizing enterocolitis (NEC).

Imaging Algorithm

Radiography

The radiographic evaluation of neonatal bowel disorders begins with a supine frontal radiograph of the abdomen. An imaging algorithm for bilious emesis, a common presenting sign of a neonatal bowel emergency, is presented in Figure 1. If esophageal pathologies are suspected, the chest may also be included in the examination. If there is clinical concern for perforation, ischemia, or obstruction, a left lateral decubitus or cross-table lateral view may be obtained to evaluate for free intraperitoneal or portal venous gas and differential air-fluid levels. Rectal gas is best assessed with a prone view. In the setting of obstruction, the initial abdominal radiographs, in combination with clinical symptoms, help differentiate proximal from distal bowel obstructions. When possible, monitoring equipment and the comfort pads should be removed from the FOV to optimize radiographic evaluation and reduce radiation dose [1, 2].

Certain neonatal bowel disorders have a pathognomonic appearance on conventional radiographs, precluding the need for further imaging. For example, in the setting of isolated EA or EA with proximal TEF (Gross types A and B), radiographs show a gasless abdomen. A double bubble on conventional radiographs refers to the gaseous distention of the stomach and a dilated duodenal bulb, and is diagnostic of duodenal atresia [3]. A triple bubble refers to the characteristic additional gaseous distention of a third hollow viscous—that is, a dilated proximal jejunal loop—related to a proximal jejunal atresia [3].

Fluoroscopy

After conventional radiographs, a fluoroscopic upper GI series (UGI) is the next step in the radiologic evaluation of the esophagus, stomach, and proximal small bowel. Suspected malrotation requires an emergent UGI, because findings on radiographs can be normal. A UGI may also elucidate the anatomy of upper intestinal obstruction when conventional radiographs are indeterminate [3]. For neonates, a UGI is performed with the patient recumbent while lateral and frontal projections of the esophagus, stomach, and duodenum are obtained. In certain cases,

Keywords: bowel, malrotation, microcolon, neonatal, obstruction

doi.org/10.2214/AJR.17.19378

Received December 6, 2017; accepted after revision January 5, 2018.

[1]All authors: Department of Radiology, Seattle Children's Hospital, University of Washington School of Medicine, 4800 Sand Point Way NE, Seattle, WA 98105. Address correspondence to G. S. Phillips (grace.phillips@seattlechildrens.org).

This article is available for credit.

AJR 2018; 210:976–988

0361–803X/18/2105–976

placement of a nasoenteric tube may assist in control of the contrast bolus. When there is concern for TEF, the patient is ideally positioned prone, and contrast agent is instilled into the esophagus in the lateral projection. Of note, prone imaging in the lateral projection requires use of a mobile C-arm positioner fluoroscopy unit.

To exclude malrotation, meticulous technique, with both frontal and lateral projections, is required (Fig. 2). Attention must be paid to patient positioning so that frontal and lateral projections are obtained without obliquity. To study the gastric outlet and duodenum, the patient is placed in the right lateral decubitus position until contrast agent distends the second portion of the duodenum. The patient is then positioned supine to document the duodenal-jejunal junction in the frontal projection. The patient may then be placed in the right lateral decubitus position a second time to document the location of the fourth portion of the duodenum. A normal lateral projection of the duodenum shows a posterior or retroperitoneal location of both the proximal and distal portions of the duodenum. A normal frontal projection confirms that the duodenal-jejunal junction is to the left of the spine at the level of the pylorus. Ideally, the first bolus of contrast agent is imaged as it passes through the duodenum, because contrast-filled loops of jejunum may obscure the course of the duodenum on subsequent boluses.

Enemas with contrast material (CE) are used to define the anatomy of the rectum, colon, and distal small bowel, often in the setting of suspected distal obstruction. A soft-tipped catheter is inserted into the rectum, and contrast agent is instilled retrograde. Both lateral and frontal rectal images are important to obtain if HD or anorectal malformation is suspected. The study is considered complete once opacification of the cecum or distal small bowel is achieved. Full distention of the colon may be impossible in the setting of colonic atresia.

With both UGI and contrast enema examinations, adherence to the ALARA (as low as reasonably achievable) principle helps to mitigate patient radiation exposure. Suggested methods to reduce radiation dose to the patient include using intermittent pulsed fluoroscopy, last image capture, and appropriate collimation; removing the antiscatter grid; avoiding digital magnification; and shortening the distance between the patient and the image intensifier.

Ultrasound, CT, and MRI

In recent years, the role of ultrasound has become increasingly defined for particular neonatal bowel disorders. Ultrasound is the mainstay for diagnosis in suspected pyloric stenosis, with a sensitivity and specificity that approach 100% [4–6]. With respect to NEC, sonography complements conventional radiography by providing a real-time assessment of bowel peristalsis, perfusion, and wall thickness, as well as characterization of peritoneal fluid [6–8]. UGI remains the study of choice for suspected malrotation [6]. Cystic abdominal masses, such as bowel duplication cysts, meconium pseudocysts, and mesenteric cysts, are well depicted by sonography.

CT and MRI are infrequently used to assess neonatal bowel disorders because of the inherent radiation dose related to CT and potential need for sedation for MRI examinations. However, in complex cases, these modalities may be used for problem solving. As MRI technology advances, the potential for MRI without sedation using fast MRI sequences may expand its role. A recent study showed the feasibility of high-resolution MRI without sedation in infants up to age 4 months with anorectal malformations [9].

Upper Intestinal Neonatal Bowel Disorders

Esophageal Atresia and Tracheoesophageal Fistula

EA may be seen in isolation or in association with a TEF. EA has an estimated frequency of 1 in 2500–3000 live births [10]. TEFs may be classified on the basis of their anatomic location and configuration using the Gross classification (Fig. 3), which includes the following: type A, isolated EA; type B, EA with a proximal TEF; type C, EA with a distal TEF; type D, EA with both proximal and distal TEFs; and type E, TEF without EA [11]. Patients with EA, including up to 65% without TEF, may have additional anomalies of the cardiovascular, musculoskeletal, gastrointestinal, and genitourinary systems [11]. The designation "VACTERL" is defined as three or more anomalies of the vertebral, anorectal, cardiac, tracheal, esophageal, renal, and limb systems without a chromosomal aberration.

Prenatal sonography of fetuses with EA may show polyhydramnios and absence of the stomach bubble. If EA is undiagnosed prenatally, patients typically present in the early postnatal period with feeding difficulties, drooling, and cyanosis or apnea while feeding [11]. At clinical examination, the inability to place a nasogastric tube may be diagnostic. Neonates with isolated EA, or EA with a proximal TEF, will have an absence of abdominal bowel gas on conventional radiographs. With a distal TEF, although the abdomen may initially be gasless, bowel gas is typically seen after 4 hours of life [12]. Bronchoscopy is considered the diagnostic test of choice for TEF in the setting of EA [13, 14]. UGI examination is generally contraindicated in EA because of the risk of aspiration [15]. After surgical repair, UGI can help diagnose complications such as anastomotic leak, which is seen in 15–20% of patients, and stricture formation, which is present in 30–40% of these patients [11].

Hypertrophic Pyloric Stenosis

Hypertrophic pyloric stenosis (HPS) is a form of gastric outlet obstruction due to abnormal thickening and elongation of the pylorus. Although the exact cause of HPS is unclear, both environmental and genetic factors likely contribute to its development. Male sex, primiparity, prematurity between 28–36 weeks' gestational age, and postnatal erythromycin exposure are recognized risk factors [16]. In addition, five genetic loci have been associated with HPS [16]. HPS typically presents between 2 and 12 weeks of age with nonbilious projectile emesis [16]. The classic physical examination sign of a palpable "olive" related to the thickened elongated pyloric channel has become less common, likely because of earlier diagnosis [17].

In the past, before the refinement of ultrasound, UGI was used to diagnose HPS. At UGI, contrast agent within a narrowed elongated pyloric channel results in a "string" sign (Fig. 4A). The impression of the thickened muscular channel on the antrum or duodenum creates the shoulder and mushroom signs, respectively. Dynamic evaluation of the stomach reveals hyperperistalsis of the stomach with minimal egress of contrast agent. Ultrasound has replaced UGI as the study of choice for suspected HPS because of its high sensitivity and specificity and lack of ionizing radiation. In HPS, the single muscular wall thickness measures greater than or equal to 3 mm, and the pyloric channel length measures greater than or equal to 15 mm [18] (Fig. 4B). Imaging in the right lateral decubitus position may help to mitigate a limited acoustic window from a gaseously overdistended stomach [16]. As

with UGI, gastric emptying may be assessed with ultrasound dynamically. Pylorospasm, which is a temporary closing of the pyloric channel due to muscle spasm, is a pitfall in diagnosis. Pylorospasm can be excluded by prolonged or repeat imaging [16]. At our institution, we reimage the pylorus with ultrasound after 20–30 minutes if pylorospasm is initially suspected.

Duodenal Obstruction and Duodenal Atresia

Duodenal atresia results from failure of gut recanalization during embryologic development, which causes a complete obstruction. Duodenal atresia may be seen as an isolated finding or in association with trisomy 21. At prenatal sonography, polyhydramnios in combination with a double bubble may be present, with fluid distending a dilated stomach and proximal duodenum. Common presenting symptoms in the undiagnosed neonate are bilious or nonbilious emesis. The characteristic radiographic double bubble sign is diagnostic of duodenal atresia in neonates (Fig. 5), signifying a gas-filled dilated stomach and duodenal bulb. Although the remainder of the abdomen is typically gasless, rarely distal gas is seen if an anomalous biliary duct joins the duodenum on both sides of the atretic duodenal segment [19]. In this case, a UGI may confirm the diagnosis of duodenal atresia.

Duodenal Stenosis and Duodenal Web

In contrast to duodenal atresia, duodenal stenosis and web are partially obstructing lesions. As the name implies, duodenal stenosis is a narrowed (typically second) segment, as can be seen at UGI, related to incomplete recanalization. A duodenal web is a thin membrane that partially obstructs and also usually occurs in the second segment of the duodenum, at the level of the ampulla of Vater [20]. At UGI examination, a duodenal web may show a windsock deformity, as contrast agent distends a dilated proximal duodenum and outlines a thin web that bulges into the nondilated distal segment. A windsock deformity may also be seen sonographically if the distal segment is fluid- or gas-filled, which allows the differentiation between a duodenal web and duodenal atresia [20]. Of note, duodenal stenosis and web are strongly associated with malrotation, annular pancreas, and a preduodenal portal vein, which should be considered in the differential diagnosis of partial or complete duodenal obstruction.

Malrotation

Malrotation or intestinal rotation anomalies are a spectrum of conditions caused by absent or incomplete bowel rotation during the embryologic process of bowel rotation, which may also lead to abnormal bowel fixation [21]. These conditions can be classified as true malrotation, atypical malrotation, and nonrotation [22]. True malrotation implies an abnormal position of the duodenojejunal junction or ligament of Treitz in the right upper quadrant associated with a high-riding cecum in the mid or upper abdomen, with a resultant narrow mesenteric pedicle that can predispose the patient to potentially catastrophic midgut volvulus and bowel ischemia. During embryologic development, attempts at fixation of the abnormally positioned cecum will lead to formation of aberrant adhesive peritoneal bands (Ladd bands) that extend from the cecum toward the right abdominal wall. These bands can overlay the duodenum and potentially cause duodenal obstruction [23, 24].

In patients with atypical malrotation, the ligament of Treitz is at or to the left of midline but below the level of the pylorus and may be associated with a high-riding or mobile cecum [22, 25, 26]. If atypical malrotation is incidentally diagnosed in older patients without symptoms, observation is thought to be appropriate for management, whereas surgery may be considered in asymptomatic younger patients [22].

Nonrotation represents an incidental finding present in 2% of UGI studies [27] and is defined by the absence of embryologic bowel rotation, with the small bowel positioned in the right abdomen, whereas the colon will be located on the left. In nonrotation, the mesenteric root is broad, leading to a low risk of midgut volvulus [24, 28, 29].

The true incidence of malrotation remains unknown because many patients may remain clinically silent; the estimated prevalence is approximately 1 in 500 live births [30]. Congenital diaphragmatic hernia, omphalocele, and heterotaxy syndromes have a high association with malrotation. Other entities associated with malrotation include duodenal or intestinal atresia or web, biliary atresia, Meckel diverticulum, and HD [24, 31].

Bilious emesis in a neonate represents the classic clinical presentation of malrotation (Figs. 6A–6C). Cases evolving to bowel ischemia will manifest with abdominal pain, distention, hematochezia, and eventually hypovolemic or septic shock with peritonitis. UGI remains the imaging method of choice in the diagnosis of malrotation and midgut volvulus [22, 28, 31]. Diagnosis of malrotation on UGI relies on meticulous technique with documentation of the duodenal course achieved on both frontal and lateral views, as discussed earlier in the Fluoroscopy section, ideally during the first bolus of contrast agent, because opacification of proximal jejunal loops may obscure the duodenal segments and compromise the examination [28]. Findings diagnostic for true malrotation include abnormal position of the duodenojejunal junction to the right of the spine and proximal jejunal loops located in the right upper abdomen. Of note, right-sided jejunal loops without other associated abnormalities represent a normal anatomic variant in 2% of patients [32].

In midgut volvulus, there is a corkscrew configuration of the duodenum with a tapered or beaked appearance [28]. Up to 15% of UGI examinations may lead to false-positive results of malrotation, most commonly due to unrecognized anatomic variants such as duodenal redundancy or duodenum inversum [31]. Duodenum inversum (Fig. 7) is a rare, usually asymptomatic, congenital condition characterized by a superior and posterior track of the third duodenum before crossing the midline at a high level above the pancreas toward the ligament of Treitz, which is usually in a normal position [33, 34]. Duodenal redundancy or wandering duodenum (Fig. 8) will present with a meandering course of the proximal duodenum, which may form one or multiple loops to the right of the spine, but crossing the midline at a normal level and also with a normal position of the ligament of Treitz [31, 34].

In addition, malrotation may be misdiagnosed in the setting of apparent displacement of the duodenojejunal junction, which may be present in children younger than 4 years due to ligamentous laxity, in patients with indwelling entering tubes, or due to mass effect from liver transplant, splenomegaly, or renal or retroperitoneal tumors [24, 28, 31]. The duodenal-jejunal junction may also be displaced in the setting of a distended stomach, small bowel, or colon. If UGI results are not definitive for the diagnosis of malrotation, a small-bowel follow-through or CE may be performed, depending on the patient's clinical status, to evaluate the cecal position, from which one may infer the length of mesentery. The position of the cecum is however normal in 20% of cases of malrotation [35, 36].

Lower Gastrointestinal Neonatal Bowel Disorders

Jejunoileal Atresia

Jejunoileal atresia is thought to arise from intrauterine vascular insult, which results in necrosis and resorption, leading to segmental stenosis. The frequency is estimated at 1 in every 3000–5000 live births [37]. Clinical presentation is early in life and is characterized by bilious emesis in proximal atresia and abdominal distention and failure to pass meconium in distal atresia.

Radiographic appearance is dependent on the site of obstruction and timing of prenatal injury. In proximal jejunal atresia, the classic appearance is a triple bubble, with gaseous distention of the stomach, duodenum, and proximal jejunum (Fig. 9). This is in contradistinction to distal atresia, which is characterized by numerous distended loops of bowel (Fig. 10A). Multiple or long-segment atresias can have a mixed appearance. Regardless of the location of small-bowel atresia, peritoneal calcifications may be present secondary to in utero perforation and meconium peritonitis.

UGI may be considered for proximal atresia, and CE is indicated for suspected distal atresia. However, in either case, the examinations may be complementary to exclude an additional distal stenosis or atresia in the former scenario, or malrotation in the clinical presence of bilious emesis in the latter scenario. As with conventional radiographs, the fluoroscopic appearance can be variable and is dependent on the location of the atresia. Microcolon is defined as a diffusely small caliber, but normal in length, colon (Fig. 10B) and results from a functionally unused or underutilized colon. Microcolon is the typical finding on CE for distal small bowel (ileal) and multiple or segmental atresias. Conversely, proximal jejunal atresia can present with a normal appearance of the colon on CE. This is due to a larger length of small bowel that is in continuity to the colon, resulting in a normal utilized appearance.

Meconium Ileus

Meconium ileus is neonatal obstruction of the distal ileum due to abnormally thick and tenacious meconium. Up to 90% of full-term neonates with meconium ileus have cystic fibrosis [38]. The frequency of cystic fibrosis is 1 in 3500 white live births [39]; it is much rarer in patients of other races. The pathophysiology of cystic fibrosis is genetic mutation in the *CFTR* gene, which alters cellular chloride ion exchange and leads to dehydration of the intraluminal contents, resulting in thickened meconium.

Uncomplicated or simple cases of meconium ileus present radiographically as a typical distal small-bowel obstruction with dilated upstream bowel. Complicated cases of meconium ileus are defined by the presence of segmental volvulus, atresia, necrosis, or perforation [40] and can have a more variable radiographic appearance. In the case of necrosis or perforation, the leak of meconium causes an inflammatory response leading to meconium peritonitis, which manifests as peritoneal calcifications and, when walled off, leads to meconium pseudocyst formation. The meconium peritoneal calcifications can be detected either radiographically or sonographically. However, pseudocyst formation is best characterized by ultrasound (Fig. 11). A mesenteric pseudocyst can be singular or multiple and may have thickened walls with irregular septations and associated mural calcifications.

On CE, similar to distal small bowel atresia, meconium ileus will present with a microcolon. However, when contrast material is refluxed into the terminal ileum, multiple characteristic filling defects representative of the tenacious meconium are present. The use of water-soluble contrast agent, rather than barium, is important in this entity because it is both diagnostic and potentially therapeutic. Water-soluble contrast agents vary in osmolality. In the clinical scenario of meconium ileus, a contrast agent that is hyperosmotic to plasma is preferred for therapeutic reasons because it will draw water into the lumen of the bowel, aiding the disimpaction. Diatrizoate meglumine and diatrizoate sodium (Gastrografin, Bracco Diagnostics) is highly hyperosmotic (1940 mOsm/kg water) compared with other water-soluble agents, such as iothalamate meglumine (400 mOsm/kg water; Cysto-Conray II, Mallinckrodt), and care must be taken to ensure that the child is adequately hydrated, if diatrizoate meglumine with diatrizoate sodium is used. In simple cases of meconium ileus, the published success rates for disimpaction with water-soluble enemas is 5–83% [40].

Imperforate Anus and Colonic Atresia

Imperforate anus is usually clinically evident and may be diagnosed by prenatal ultrasound secondary to dilation of upstream bowel. Other less common prenatal ultrasound findings of anal atresia are failure to demonstrate the anus and enteroliths, which are calcifications of the meconium caused by mixing of urine secondary to associated genitourinary anomalies [41, 42]. The estimated incidence of anorectal malformation is 1 in 2500–5000 live births [43]. There is an association with trisomy 18 and 21 and VACTERL syndromes; however, most cases are sporadic.

Radiographically, the appearance is similar to that of other distal obstructions with dilated upstream bowel loops. Although a CE cannot be performed, a voiding cystourethrogram may be performed to evaluate for associated genitourinary tract anomalies. Management typically involves an upstream colostomy and mucous fistula distally. Before attempted creation of a neorectum, fluoroscopy of the mucous fistula may be useful for presurgical planning. This evaluation variably shows an unused appearance of the distal colon and can reveal additional associated genitourinary anomalies, such as fistulas (Fig. 12).

Colonic atresia is a rare disease with an incidence of 1 in 66,000 live births [44]. The three types described in the literature [45] are a colonic membrane (type 1), discontinuity of colon with a fibrous band and an intact mesentery (type 2), and separated colon with a mesenteric defect (type 3). As with anal atresia, this entity can be detected on prenatal ultrasound with dilated fluid filled upstream bowel.

Classically, colonic atresia will appear similar to other distal obstructions by conventional radiographic evaluation. At fluoroscopic evaluation, the three types are generally indistinguishable, with an abrupt cutoff of the colon typically shown. However, type 1 colonic atresia can have a pathognomonic windsock sign due to the contrast material distending or bulging the pathologic membrane [46].

Functional Immaturity of the Colon

Functional immaturity of the colon is also known as "small left colon syndrome" and "meconium plug syndrome." The latter term may cause confusion because meconium plugs located in the terminal ileum are referred to as "meconium ileus," as discussed already. Functional immaturity of the colon is, however, a transient obstruction of the distal colon. In this entity, the meconium material is in the colon, not the terminal ileum, and it is not the underlying cause of the obstruction but a consequence of the functional obstruction. The cause of the functional obstruction is unclear but is thought to be secondary to

immaturity of the ganglion cells or hormone receptors. The frequency is higher in children of diabetic mothers and neonates of mothers who receive magnesium sulfate as part of the treatment for preeclampsia [47]. These neonates typically present with delayed passage of meconium and abdominal distention. The prognosis is excellent in these cases, and the symptoms typically resolve in a few days.

On conventional radiographs, there can be multiple dilated segments of bowel, similar to other distal obstructions, such as ileal atresia and meconium ileus. However, in utero bowel perforation has not been reported, and thus peritoneal calcifications have not been described. On CE, a microcolon should not be present. As the alternative name of "small left colon syndrome" implies, only the distal colon will be small, which is distinctly different from microcolon, which is a diffuse process involving the entire colon. Although the distal colon is small, the rectosigmoid ratio should remain normal (Fig. 13). Contrast typically outlines meconium plugs within the colon.

Hirschsprung Disease

HD is a congenital disorder of the enteric nervous system. The incidence is 1 in every 5000 live births [48]. There is a 2.5:1 to 5:1 male predilection. Approximately 3–8% of cases are familial, with multiple mutations identified [49]. It is characterized by absence of the ganglion cells of the myenteric and submucosal plexus of the rectum and colon. The aganglionic segment lacks the signal to relax and, thus, is in a constant state of spasm. Neonates typically present with failure to pass meconium and abdominal distention. Although the fluoroscopic findings may be suggestive of the diagnosis, imaging alone cannot exclude HD, and suction biopsy is required for definitive diagnosis.

On conventional radiographs, there is gaseous distention of numerous loops of bowel, similar to the other distal obstructions already discussed. CE classically shows a rectosigmoid diameter ratio of less than 1. However as previously stated, a rectosigmoid ratio greater than 1 does not exclude HD. CE remains an important diagnostic test for neonates with suspected HD to evaluate for other causes of distal obstructions and for preoperative planning. If present, HD nearly always affects the distal rectum, and more proximal contiguous colonic segments are variably affected. A transition point is often identified with upstream dilation (Fig. 14), which may mimic the appearance of small left colon syndrome, but the rectosigmoid ratio is usually normal (> 1) in small left colon syndrome. Although a transition point may be present at imaging, correlation with pathologic aganglionosis is sporadic. Jamieson et al. [50] showed an overall concordance of 62.5% between imaging and pathologic analysis and, in a subgroup of long-segment HD, a concordance of only 25%. A sawtooth pattern of the distal rectum may be seen at fluoroscopy, representing spasm secondary to aganglionosis. Total colonic HD may have an appearance similar to that of microcolon, although a more rounded configuration of the colon creating a question mark– or comma-shaped colon has been described [51].

Necrotizing Enterocolitis

Despite a gradual decrease in incidence over the last 10 years because of improved prevention strategies [52, 53], NEC remains the most common gastrointestinal emergency in neonatal ICUs [54]. The pathogenesis of this inflammatory bowel condition is thought to be multifactorial, with immature bowel function, bowel hypoxia or ischemia, type of enteral feeding, and disruption of gut microbiota likely representing contributing factors [52, 54–56]. NEC remains primarily a disease of premature infants, especially those with birth weight below 1500 g [7, 57, 58]. However, approximately 10% of cases are seen in full-term neonates [59], with up to one-third of these cases presenting in association with congenital heart disease, particularly entities predisposing to alterations of bowel perfusion, such as left ventricular outflow lesions or single ventricle physiology [60–62]. The classic presentation of NEC in premature infants includes abdominal distention, feeding intolerance, and bloody stools. In premature infants, NEC typically occurs in the second or third week of life [63]. In contrast, NEC tends to manifest earlier in full-term neonates, during the first week of life [64, 65].

Imaging with radiography and ultrasound plays an essential role in the diagnosis of NEC, as well as in monitoring disease progression. Radiography remains the imaging modality of choice, with abdominal radiographs performed every 6 hours [66] during the NEC watch until remission of symptoms and finding, or progression is seen. The bowel gas pattern in NEC can include various findings, ranging from diffuse nonspecific gaseous distention due to ileus [7, 67] to fixed dilated loops of bowel, thought to represent an impending sign of perforation from full-thickness wall necrosis, to a completely gasless abdomen in the setting of dilated bowel loops filled with fluid [68, 69]. Pneumatosis, with curvilinear or bubbly lucencies paralleling the bowel wall, represents a pathognomonic sign for NEC. Pneumatosis frequently involves the right lower quadrant within distal small bowel and proximal colonic walls, although it may occur in any location along the gastrointestinal tract [7]. Portal venous gas may be transient and indicates progression to severe disease [70]. Although portal venous gas is not an indication for surgical intervention, it is significantly associated with the eventual need for surgery [69]. Pneumoperitoneum (Fig. 15) remains an absolute indication for surgery and indicates bowel necrosis with perforation. Of note, pneumoperitoneum is absent in more than half of patients with perforation and necrosis [7, 71–73].

The role of ultrasound in NEC varies from institution to institution and is operator dependent. Ultrasound does have the potential to provide very useful additional information beyond radiographs alone, particularly in centers with experience. Ultrasound has advantages over radiographs that include real-time evaluation of bowel peristalsis, wall thickness, and perfusion. As such, ultrasound allows diagnosis of NEC in early stages, showing increased bowel wall thickening, increased perfusion, and initial pneumatosis at a time when radiographs typically show nonspecific bowel distention [66]. In addition, portal venous gas and pneumoperitoneum can be seen at sonography with at least a similar sensitivity as radiographs [7, 74]. Adverse outcomes may be predicted when abnormal bowel thickness measures above 2.8 mm or below 1.1 mm, or when aperistalsis and absent perfusion, with or without complex free fluid, are detected on ultrasound [69, 74].

Conclusion

Radiology plays a fundamental role in the diagnosis of neonatal bowel disorders, as summarized in Table 1. Prompt diagnosis of these potentially life-threatening conditions requires a methodical diagnostic approach and familiarity with radiographic and fluoroscopic patterns of disease. Although some entities may be diagnosed by prenatal ultrasound or MRI, postnatally radiographs and fluoroscopy remain the cornerstones of diagnostic imaging for many neonatal bowel disorders. The exception is HPS, in which ultrasound has essentially replaced UGI ex-

TABLE 1: Role of Radiology in Diagnosing Neonatal Bowel Disorders

Type of Disorder	Diagnostic Test	Imaging Findings	Pitfalls in Diagnosis and Additional Considerations	Current Management
Tracheoesophageal fistula	UGI examination	Fistulous connection between esophagus and trachea; refer to Figure 3 for types of TEF	UGI examination may miss TEFs even with meticulous technique	Surgical repair
Hypertrophic pyloric stenosis	Ultrasound	Persistent abnormal thickening (> 3 mm) and elongation (> 15 mm) of the pyloric channel	Pylorospasm can mimic pyloric stenosis; consider repeat imaging if pylorospasm is suspected	Pyloromyotomy
Duodenal atresia	Abdominal radiographs	Double bubble: gaseous distention and dilation of the stomach and duodenum	Rarely distal gas is seen if an anomalous biliary duct joins the duodenum on both sides of the atretic duodenal segment	Duodenoduodenostomy
Duodenal stenosis	UGI examination	Narrowed, typically second duodenal segment	Strongly associated with malrotation, annular pancreas, and a preduodenal portal vein	Duodenoduodenostomy
Duodenal web	UGI examination	Windsock deformity, as contrast agent distends a dilated proximal duodenum, and outlines a thin web that bulges into the nondilated distal segment	Strongly associated with malrotation, annular pancreas, and a preduodenal portal vein	Duodenoduodenostomy; resection of web
Malrotation	UGI examination	Abnormal position of the duodenal-jejunal junction	Duodenum inversum; duodenal redundancy; displacement of the duodenal-jejunal junction due to ligamentous laxity, in patients with indwelling enteric tubes or due to mass effect from liver transplant, splenomegaly or renal or retroperitoneal tumors, a distended stomach, small bowel, or colon	Ladd procedure
Proximal jejunal atresia	Radiographs; UGI examination	Triple bubble sign on radiographs, with gaseous distention of the stomach, duodenum, and proximal jejunum; UGI appearance is variable depending on site of atresia	Multiple or long-segment atresias can have a mixed appearance	Surgical resection of the atretic segment(s)
Distal ileal atresia	Contrast enema	Microcolon	Multiple or long-segment atresias can have a mixed appearance	Surgical resection of the atretic segment(s)
Meconium ileus	Contrast enema	Microcolon; when contrast material is refluxed into the terminal ileum, multiple characteristic filling defects representing tenacious meconium are present	Complicated cases of meconium ileus are defined by the presence of segmental volvulus, atresia, necrosis, or perforation, and can have a more variable radiographic appearance; peritoneal calcifications and pseudocyst formation (best characterized by ultrasound) may occur	Enema may be therapeutic
Imperforate anus	Physical examination; radiographs	Distal bowel obstruction	Voiding cystourethrogram may be performed to evaluate for associated genitourinary tract anomalies	Colostomy before definitive surgical repair
Colonic atresia	Radiographs; contrast enema	Distal bowel obstruction on radiographs; abrupt cutoff of the colon on enema	On fluoroscopic evaluation the three types are generally indistinguishable, although type 1 colonic atresia can have a pathognomonic windsock sign due to the contrast material distending or bulging the pathologic membrane	Colostomy before definitive surgical procedure
Functional immaturity of the colon	Radiographs; contrast enema	Distal bowel obstruction by radiographs; on enema, the distal colon will be small and the rectosigmoid ratio is normal; contrast material typically outlines meconium plugs within the colon	Microcolon should not be present	Supportive care

(Table 1 continues on next page)

TABLE 1: Role of Radiology in Diagnosing Neonatal Bowel Disorders (continued)

Type of Disorder	Diagnostic Test	Imaging Findings	Pitfalls in Diagnosis and Additional Considerations	Current Management
Hirschsprung disease	Abdominal radiographs; contrast enema	Distal bowel obstruction by radiographs; at enema with contrast material, rectosigmoid ratio should be < 1; transition point is often identified with upstream dilation; sawtooth pattern of the distal rectum; total colonic Hirschsprung disease may have a similar appearance to microcolon	Enema can be normal; rectal biopsy is reference standard	Surgical resection of aganglionic segment
Necrotizing enterocolitis	Abdominal radiographs; ultrasound	On radiographs, pneumatosis, portal venous gas, and free intraperitoneal air are seen; ultrasound in early stages shows increased bowel wall thickening, increased perfusion and initial pneumatosis; ultrasound may also show portal venous gas and pneumoperitoneum.	The bowel gas pattern in necrotizing enterocolitis can include various findings ranging from diffuse nonspecific gaseous distention due to ileus to fixed dilated loops of bowel, thought to represent an impending sign of perforation from full thickness wall necrosis, to a completely gasless abdomen in the setting of dilated bowel loops filled with fluid	Supportive care; surgical management for perforation

Note—UGI = upper gastrointestinal, TEF = tracheoesophageal fistula.

amination for diagnosis. Furthermore, the role of ultrasound in NEC has expanded in recent years. We reviewed the key radiologic features of neonatal bowel disorders that will facilitate prompt diagnosis.

References

1. Rattan AS, Cohen MD. Removal of comfort pads underneath babies. *Acad Radiol* 2013; 20:1297–1300
2. Jiang X, Baad M, Reiser I, Feinstein KA, Lu Z. Effect of comfort pads and incubator design on neonatal radiography. *Pediatr Radiol* 2016; 46:112–118
3. Maxfield CM, Bartz BH, Shaffer JL. A pattern-based approach to bowel obstruction in the newborn. *Pediatr Radiol* 2013; 43:318–329
4. Hernanz-Schulman M, Sells LL, Ambrosino MM, Heller RM, Stein SM, Neblett WW. Hypertrophic pyloric stenosis in the infant without a palpable olive: accuracy of sonographic diagnosis. *Radiology* 1994; 193:771–776
5. Stunden RJ, LeQuesne GW, Little KE. The improved ultrasound diagnosis of hypertrophic pyloric stenosis. *Pediatr Radiol* 1986; 16:200–205
6. Hiorns MP. Gastrointestinal tract imaging in children: current techniques. *Pediatr Radiol* 2011; 41:42–54
7. Epelman M, Daneman A, Navarro OM, et al. Necrotizing enterocolitis: review of state-of-the-art imaging findings with pathologic correlation. *RadioGraphics* 2007; 27:285–305
8. Anupindi SA, Halverson M, Khwaja A, Jeckovic M, Wang X, Bellah RD. Common and uncommon applications of bowel ultrasound with pathologic correlation in children. *AJR* 2014; 202:946–959
9. Thomeer MG, Devos A, Lequin M, et al. High resolution MRI for preoperative work-up of neonates with an anorectal malformation: a direct comparison with distal pressure colostography/fistulography. *Eur Radiol* 2015; 25:3472–3479
10. Spitz L. Esophageal atresia and tracheoesophageal malformations. In: Ashcraft KW, Holcomb III GW, Murphy JP, eds. *Pediatric surgery*, 4th ed. Philadelphia, PA: Elsevier Saunders, 2005:352–370
11. Pinheiro PFM. Current knowledge on esophageal atresia. *World J Gastroenterol* 2012; 18:3662–3672
12. Gedicke MM, Gopal M, Spicer R. A gasless abdomen does not exclude distal tracheoesophageal fistula: the value of a repeat x-ray. *J Pediatr Surg* 2007; 42:576–577
13. Guo W, Li Y, Jiao A, Peng Y, Hou D, Chen Y. Tracheoesophageal fistula after primary repair of type C esophageal atresia in the neonatal period: recurrent or missed second congenital fistula. *J Pediatr Surg* 2010; 45:2351–2355
14. McDuffie LA, Wakeman D, Warner BW. Diagnosis of esophageal atresia with tracheoesophageal fistula: is there a need for gastrointestinal contrast? *J Pediatr* 2010; 156:852
15. Gopal M, Woodward M. Potential hazards of contrast study diagnosis of esophageal atresia. *J Pediatr Surg* 2007; 42:E9–E10
16. Ranells JD, Carver JD, Kirby RS. Infantile hypertrophic pyloric stenosis: epidemiology, genetics, and clinical update. *Adv Pediatr* 2011; 58:195–206
17. Glatstein M, Carbell G, Boddu SK, Bernardini A, Scolnik D. The changing clinical presentation of hypertrophic pyloric stenosis: the experience of a large, tertiary care pediatric hospital. *Clin Pediatr (Phila)* 2011; 50:192–195
18. Iqbal CW, Rivard DC, Mortellaro VE, Sharp SW, St. Peter SD. Evaluation of ultrasonographic parameters in the diagnosis of pyloric stenosis relative to patient age and size. *J Pediatr Surg* 2012; 47:1542–1547
19. Latzman JM, Levin TL, Nafday SM. Duodenal atresia: not always a double bubble. *Pediatr Radiol* 2014; 44:1031–1034
20. Yoon CH, Goo HW, Kim E-R, Kim KS, Pi SY. Sonographic windsock sign of a duodenal web. *Pediatr Radiol* 2001; 31:856–857
21. Stephens LR, Donoghue V, Gillick J. Radiological versus clinical evidence of malrotation, a tortuous tale: 10-year review. *Eur J Pediatr Surg* 2012; 22:238–242
22. Graziano K, Islam S, Dasgupta R, et al. Asymptomatic malrotation: diagnosis and surgical management. *J Pediatr Surg* 2015; 50:1783–1790
23. Lampl B, Levin TL, Berdon WE, Cowles RA. Malrotation and midgut volvulus: a historical review and current controversies in diagnosis and management. *Pediatr Radiol* 2009; 39:359–366
24. Langer JC. Intestinal rotation abnormalities and midgut volvulus. *Surg Clin North Am* 2017; 97:147–159
25. McVay MR, Kokoska ER, Jackson RJ, Smith SD. The changing spectrum of intestinal malrotation: diagnosis and management. *Am J Surg* 2007; 194:712–717; discussion, 718–719
26. Mehall JR, Chandler JC, Mehall RL, Jackson RJ, Wagner CW, Smith SD. Management of typical and atypical intestinal malrotation. *J Pediatr Surg* 2002; 37:1169–1172
27. Stockmann P. Malrotation. In: Oldham KT, Colombani PM, Foglia RP, Skinner MA, eds. *Principles and practice of pediatric surgery*. Philadelphia, PA: Lippincott, Williams & Wilkins, 2005:1283–1296
28. Strouse PJ. Disorders of intestinal rotation and fixation ("malrotation"). *Pediatr Radiol* 2004; 34:837–851
29. Guzzetta PC Jr. Malrotation, volvulus, and bowel obstruction. In: Evans SR, ed. *Surgical pitfalls: prevention and management*, chapter 80. Philadelphia, PA: Saunders, 2009:819–825
30. Torres AM, Ziegler MM. Malrotation of the in-

testine. *World J Surg* 1993; 17:326–331
31. Applegate KE, Anderson JM, Klatte EC. Intestinal malrotation in children: a problem-solving approach to the upper gastrointestinal series. *RadioGraphics* 2006; 26:1485–1500
32. Sizemore AW, Rabbani KZ, Ladd A, Applegate KE. Diagnostic performance of the upper gastrointestinal series in the evaluation of children with clinically suspected malrotation. *Pediatr Radiol* 2008; 38:518–528
33. Kim ME, Fallon SC, Bisset GS, Mazziotti MV, Brandt ML. Duodenum inversum: a report and review of the literature. *J Pediatr Surg* 2013; 48:e47–e49
34. Long FR, Mutabagani KH, Caniano DA, Dumont RC. Duodenum inversum mimicking mesenteric artery syndrome. *Pediatr Radiol* 1999; 29:602–604
35. Firor HV, Harris VJ. Rotational abnormalities of the gut: re-emphasis of a neglected facet, isolated incomplete rotation of the duodenum. *Am J Roentgenol Radium Ther Nucl Med* 1974; 120:315–321
36. Morrison SC. Controversies in abdominal imaging. *Pediatr Clin North Am* 1997; 44:555–574
37. Tonni G, Grisolia G, Granese R, et al. Prenatal diagnosis of gastric and small bowel atresia: a case series and review of the literature. *J Matern Fetal Neonatal Med* 2016; 29:2753–2761
38. Kelly T, Buxbaum J. Gastrointestinal manifestations of cystic fibrosis. *Dig Dis Sci* 2015; 60:1903–1913
39. Wilmott RW, Tyson SL, Dinwiddie R, Matthew DJ. Survival rates in cystic fibrosis. *Arch Dis Child* 1983; 58:835–836
40. Karimi A, Gorter RR, Sleeboom C, Kneepkens CMF, Heij HA. Issues in the management of simple and complex meconium ileus. *Pediatr Surg Int* 2011; 27:963–968
41. Rolle U, Faber R, Robel-Tillig E, Muensterer O, Hirsch W, Till H. Bladder outlet obstruction causes fetal enterolithiasis in anorectal malformation with rectourinary fistula. *J Pediatr Surg* 2008; 43:e11–e13
42. Lam YH, Shek T, Tang MH. Sonographic features of anal atresia at 12 weeks. *Ultrasound Obstet Gynecol* 2002; 19:523–524
43. Zwink N, Jenetzky E, Brenner H. Parental risk factors and anorectal malformations: systematic review and meta-analysis. *Orphanet J Rare Dis* 2011; 6:25
44. Davenport M, Bianchi A, Doig CM, Gough DC. Colonic atresia: current results of treatment. *J R Coll Surg Edinb* 1990; 35:25–28
45. Sutton JB. Imperforate ileum. *Am J Med Sci* 1889; 98:457–461
46. Winters WD, Weinberger E, Hatch EI. Atresia of the colon in neonates: radiographic findings. *AJR* 1992; 159:1273–1276
47. Berrocal T, Lamas M, Gutiérrez J, Torres I, Prieto C, del Hoyo ML. Congenital anomalies of the small intestine, colon, and rectum. *RadioGraphics* 1999; 19:1219–1236
48. de Lorijn F, Kremer LC, Reitsma JB, Benninga MA. Diagnostic tests in Hirschsprung disease: a systematic review. *J Pediatr Gastroenterol Nutr* 2006; 42:496–505
49. Valioulis I, Aubert D, de Billy B, Bawab F, Karam R. A complex chromosomal rearrangement associated with Hirschsprung's disease: a case report with a review of the literature. *Eur J Pediatr Surg* 2000; 10:207–211
50. Jamieson D, Dundas S, Belushi S, Cooper M, Blair G. Does the transition zone reliably delineate aganglionic bowel in Hirschsprung's disease? *Pediatr Radiol* 2004; 34:811–815
51. Stranzinger E, DiPietro MA, Teitelbaum DH, Strouse PJ. Imaging of total colonic Hirschsprung disease. *Pediatr Radiol* 2008; 38:1162–1170
52. Patel AL, Panagos PG, Silvestri JM. Reducing incidence of necrotizing enterocolitis. *Clin Perinatol* 2017; 44:683–700
53. Kim JH. Necrotizing enterocolitis: the road to zero. *Semin Fetal Neonatal Med* 2014; 19:39–44
54. Zani A, Pierro A. Necrotizing enterocolitis: controversies and challenges. *F1000Res* 2015; 4:1373
55. Chen Y, Chang KT, Lian DW, et al. The role of ischemia in necrotizing enterocolitis. *J Pediatr Surg* 2016; 51:1255–1261
56. Nowicki PT. Ischemia and necrotizing enterocolitis: where, when, and how. *Semin Pediatr Surg* 2005; 14:152–158
57. Neu J, Walker WA. Necrotizing enterocolitis. *N Engl J Med* 2011; 364:255–264
58. Murthy K, Yanowitz TD, DiGeronimo R, et al. Short-term outcomes for preterm infants with surgical necrotizing enterocolitis. *J Perinatol* 2014; 34:736–740
59. Ostlie DJ, Spilde TL, St Peter SD, et al. Necrotizing enterocolitis in full-term infants. *J Pediatr Surg* 2003; 38:1039–1042
60. Polin RA, Pollack PF, Barlow B, et al. Necrotizing enterocolitis in term infants. *J Pediatr* 1976; 89:460–462
61. McElhinney DB, Hedrick HL, Bush DM, et al. Necrotizing enterocolitis in neonates with congenital heart disease: risk factors and outcomes. *Pediatrics* 2000; 106:1080–1087
62. Bolisetty S, Lui K, Oei J, Wojtulewicz J. A regional study of underlying congenital diseases in term neonates with necrotizing enterocolitis. *Acta Paediatr* 2000; 89:1226–1230
63. Kliegman RM, Fanaroff AA. Neonatal necrotizing enterocolitis: a nine-year experience. *Am J Dis Child* 1981; 135:603–607
64. Maayan-Metzger A, Itzchak A, Mazkereth R, Kuint J. Necrotizing enterocolitis in full-term infants: case-control study and review of the literature. *J Perinatol* 2004; 24:494–499
65. Ng S. Necrotizing enterocolitis in the full-term neonate. *J Paediatr Child Health* 2001; 37:1–4
66. Esposito F, Mamone R, Di Serafino M, et al. Diagnostic imaging features of necrotizing enterocolitis: a narrative review. *Quant Imaging Med Surg* 2017; 7:336–344
67. Daneman A, Woodward S, de Silva M. The radiology of neonatal necrotizing enterocolitis (NEC): a review of 47 cases and the literature. *Pediatr Radiol* 1978; 7:70–77
68. Wexler HA. The persistent loop sign in neonatal necrotizing enterocolitis: a new indication for surgical intervention? *Radiology* 1978; 126:201–204
69. He Y, Zhong Y, Yu J, Cheng C, Wang Z, Li L. Ultrasonography and radiography findings predicted the need for surgery in patients with necrotising enterocolitis without pneumoperitoneum. *Acta Paediatr* 2016; 105:e151–e155
70. Coursey CA, Hollingsworth CL, Wriston C, Beam C, Rice H, Bisset G. Radiographic predictors of disease severity in neonates and infants with necrotizing enterocolitis. *AJR* 2009; 193:1408–1413
71. Buonomo C. The radiology of necrotizing enterocolitis. *Radiol Clin North Am* 1999; 37:1187–1198
72. Munaco AJ, Veenstra MA, Brownie E, Danielson LA, Nagappala KB, Klein MD. Timing of optimal surgical intervention for neonates with necrotizing enterocolitis. *Am Surg* 2015; 81:438–443
73. Robinson JR, Rellinger EJ, Hatch LD, et al. Surgical necrotizing enterocolitis. *Semin Perinatol* 2017; 41:70–79
74. Silva CT, Daneman A, Navarro OM, et al. Correlation of sonographic findings and outcome in necrotizing enterocolitis. *Pediatr Radiol* 2007; 37:274–282

(Figures start on next page)

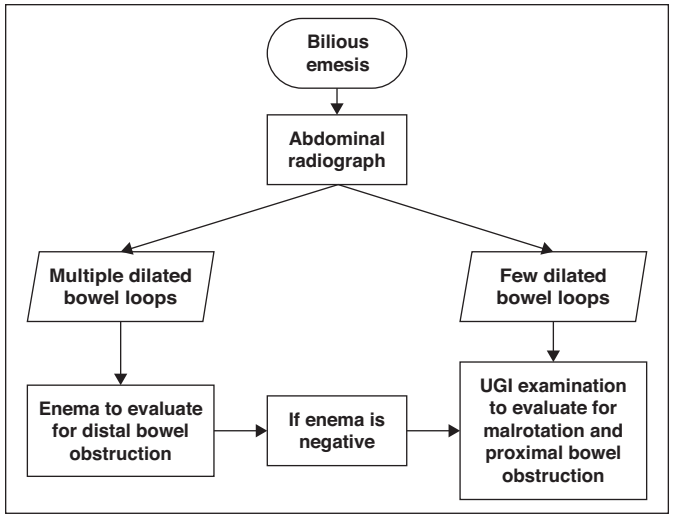

Fig. 1—Imaging algorithm for neonates presenting with bilious emesis. UGI = upper gastrointestinal series.

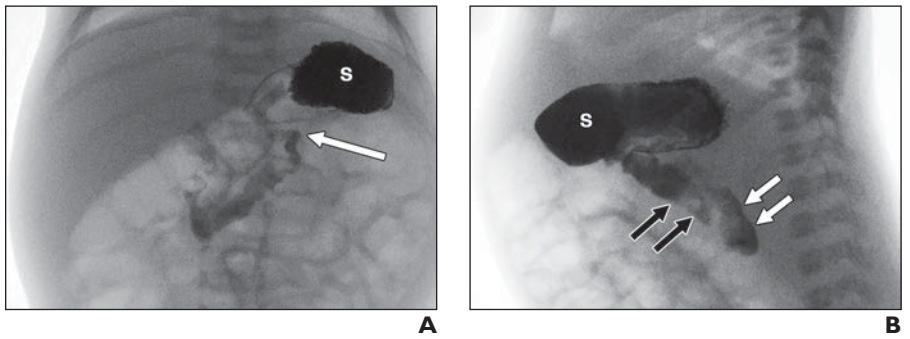

Fig. 2—14-day-old boy with bilious emesis. Contrast material is seen in stomach.
A, Frontal image from fluoroscopic upper gastrointestinal series (UGI) examination shows normal position of duodenal-jejunal junction (*arrow*), to left of spine (S) at level of pylorus.
B, Lateral image from fluoroscopic UGI examination shows normal posterior or retroperitoneal position of both second (*black arrows*) and fourth (*white arrows*) portions of duodenum.

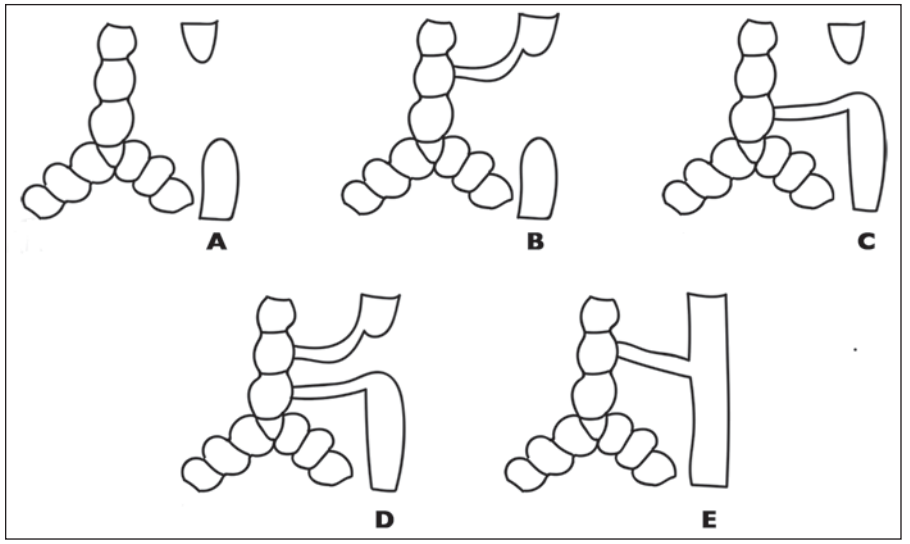

Fig. 3—Gross classification for esophageal atresia and tracheoesophageal fistulas (TEFs). (Illustrations by Phillips GS)
A–E, Schematics show type A, isolated esophageal atresia (**A**); type B, esophageal atresia with proximal TEF (**B**); type C, esophageal atresia with distal TEF (**C**); type D, esophageal atresia with both proximal and distal TEFs (**D**); and type E, TEF without esophageal atresia (**E**).

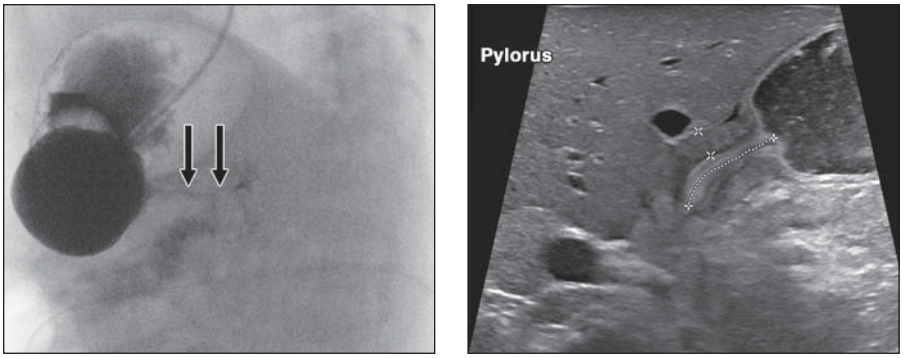

Fig. 4—3-month-old boy with pyloric stenosis.
A, Lateral image from fluoroscopic upper gastrointestinal series shows characteristic string sign of pyloric stenosis (*arrows*). Small amount of contrast material is seen passing distally.
B, Transverse sonogram shows elongated thickened pyloric channel (*dotted line*) measuring 21 mm in length with single muscular wall thickness (between *calipers*) of 5 mm, consistent with pyloric stenosis.

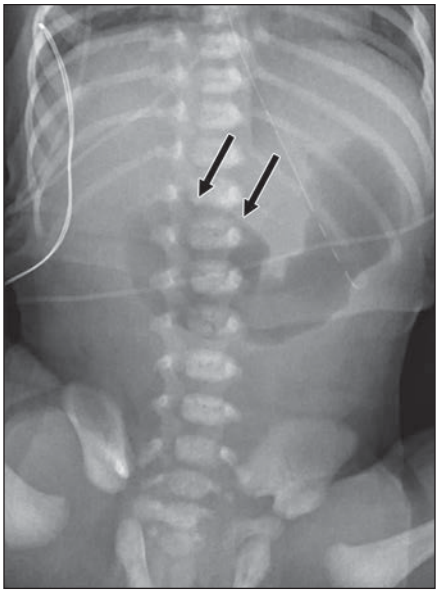

Fig. 5—3-day-old boy with duodenal atresia. Frontal radiograph shows double bubble that is pathognomonic for duodenal atresia, with pronounced dilation of gas-filled duodenal bulb (*arrows*) related to chronic obstruction. Gas-filled stomach is partially decompressed by nasogastric tube. No bowel gas is seen distal to level of obstruction.

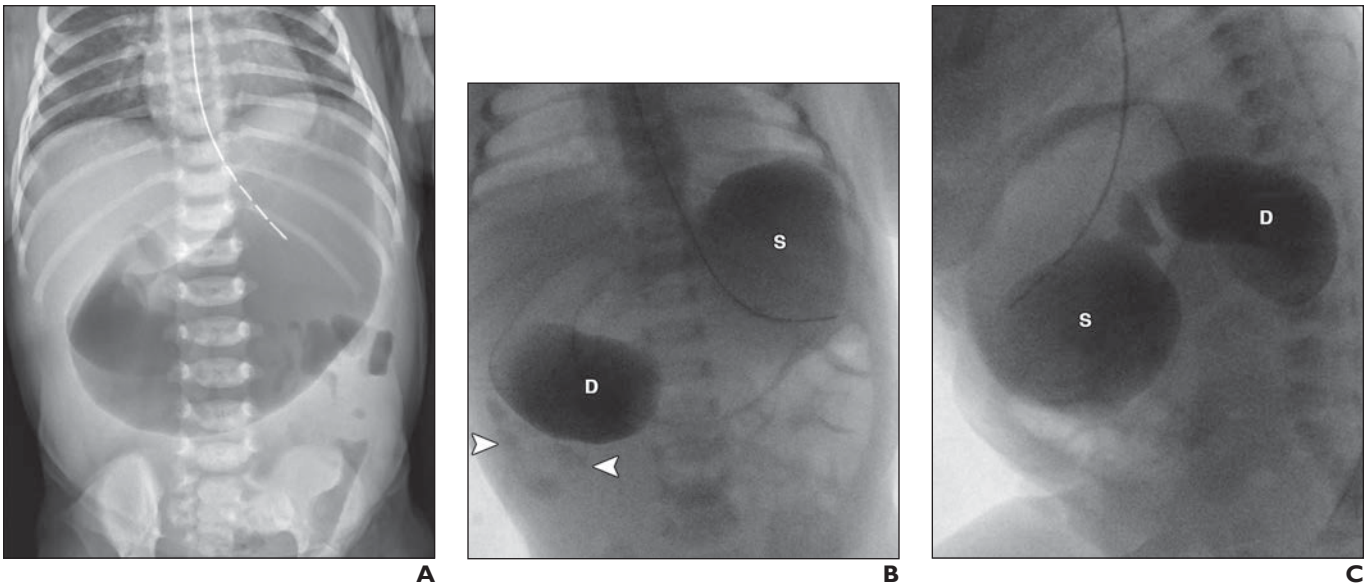

Fig. 6—6-day-old boy with malrotation and Ladd bands.
A, Frontal abdominal radiograph shows marked gaseous distention of stomach and proximal duodenum, with small amount of bowel gas seen in distal bowel loops in left hemiabdomen.
B and **C,** Frontal (**B**) and lateral (**C**) images from fluoroscopic upper gastrointestinal series again show marked distention of stomach (S) and proximal duodenum (D), with abrupt caliber change at level of transverse duodenum suspicious for mechanical bowel obstruction. There is no definite beaking or corkscrew configuration to suggest midgut volvulus. Although position of ligament of Treitz is not clearly delineated, on frontal view there is opacification of proximal small bowel loops in right hemiabdomen (*arrowheads*, **B**). Malrotation with Ladd bands was confirmed at surgery.

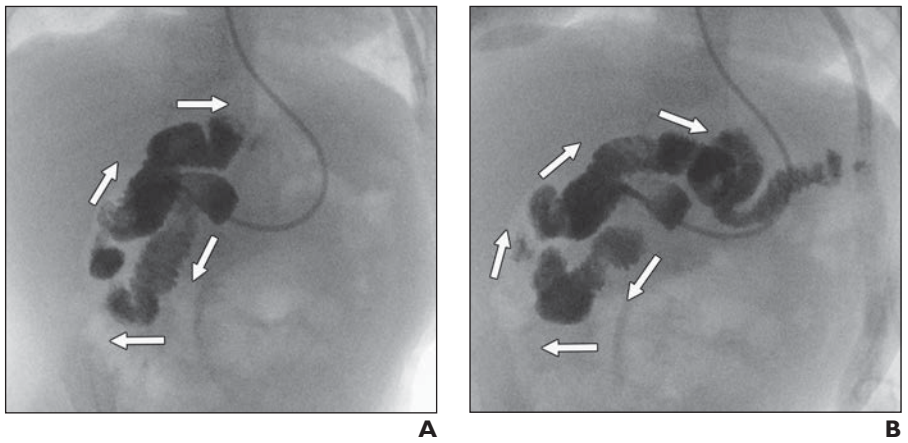

Fig. 7—4-month-old boy with duodenum inversum. **A** and **B,** Frontal serial images from fluoroscopic upper gastrointestinal series show redundant course of second and third portions of duodenum, with third portion of the duodenum with initial cephalad orientation eventually crossing midline above level of pancreas, consistent with duodenum inversum. Ligament of Treitz is to left of spine, slightly higher than duodenal bulb. Arrows outline course of duodenum.

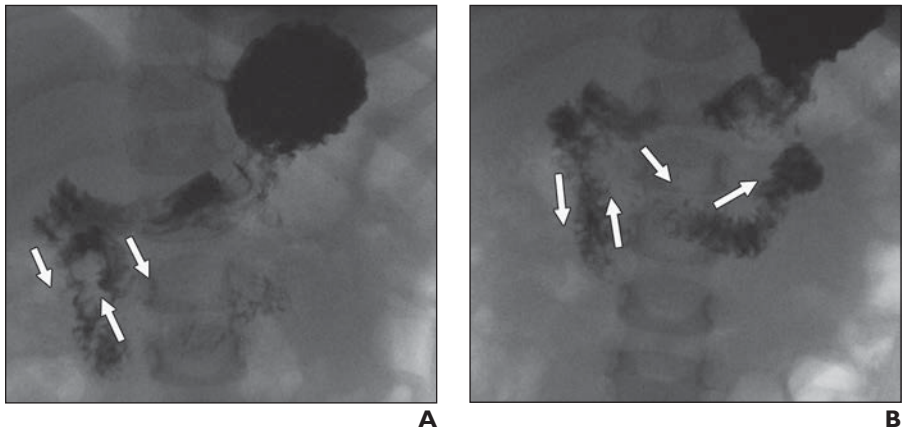

Fig. 8—2-year-old girl with duodenal redundancy. **A** and **B,** Frontal serial images from fluoroscopic upper gastrointestinal series show meandering second duodenum, with normal position of third and fourth duodenum and of ligament of Treitz. Arrows outline course of duodenum.

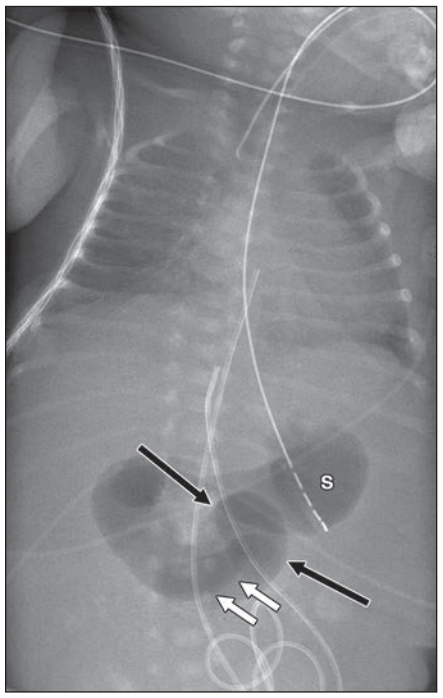

Fig. 9—2-day-old boy with proximal jejunal atresia. Frontal radiograph of chest and abdomen shows three distinct gas-filled structures representing stomach (S) and superimposed duodenum (*white arrows*) and proximal jejunum (*black arrows*).

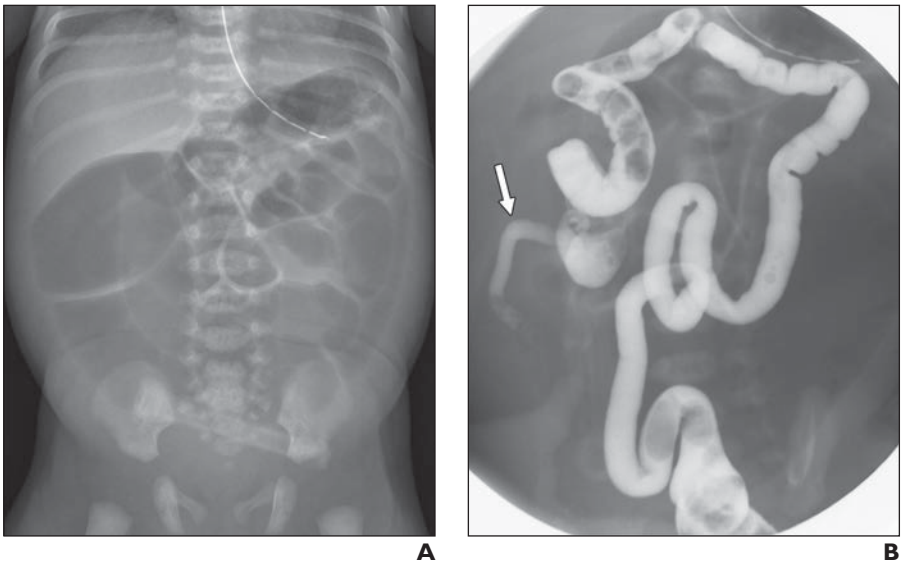

Fig. 10—0-day-old boy with ileal atresia.
A, Frontal radiograph of abdomen shows diffuse gaseous distention of multiple loops of small bowel indicative of more distal obstruction.
B, Frontal view from enema with contrast material shows diffuse small caliber of colon, consistent with microcolon. Appendix (*arrow*) is partially opacified with contrast material. Note that partially imaged rectum is wider than sigmoid colon, resulting in normal rectosigmoid ratio.

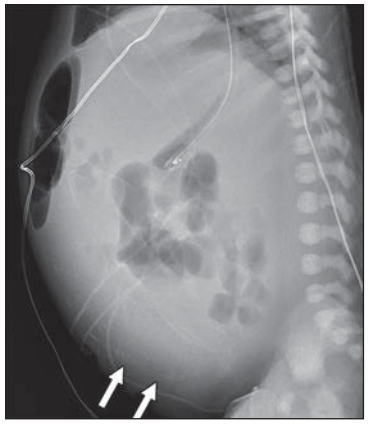

A

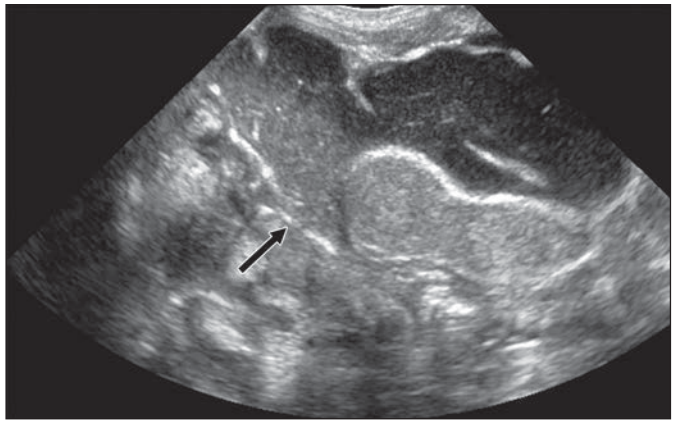

B

Fig. 11—1-day-old boy with meconium peritonitis and pseudocyst.
A, Cross-table lateral radiograph of abdomen shows distended abdomen with faint curvilinear calcifications (*arrows*) in lower anterior abdomen.
B, Transverse sonogram of right lower quadrant shows irregular cyst (*arrow*) with internal echogenic debris.

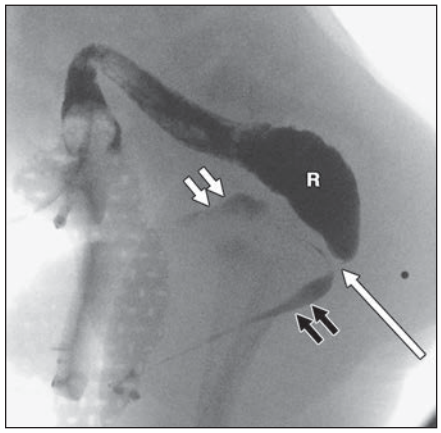

Fig. 12—7-month-old boy with imperforate anus and rectourethral fistula. Lateral view from antegrade enema with contrast material through anterior abdominal wall mucous fistula shows fistulous communication (*long white arrow*) between rectum (R) and urethra (*black arrows*), with contrast material also faintly opacifying bladder (*short white arrows*). Note that metallic BB (*black dot*) was placed at expected position of anus on perineum to aid in presurgical planning.

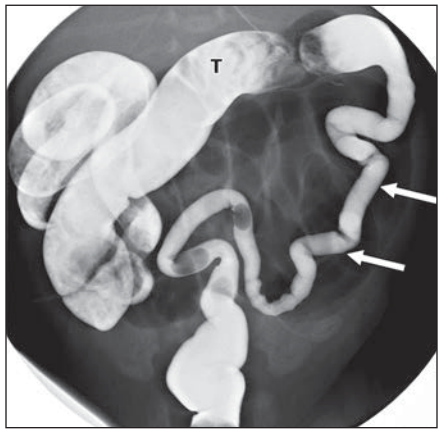

Fig. 13—1-day-old boy with functional immaturity of left colon. Frontal view from enema with contrast material shows small left colon (*arrows*). Transverse (T) and ascending colon are normal. Note that rectosigmoid ratio is normal.

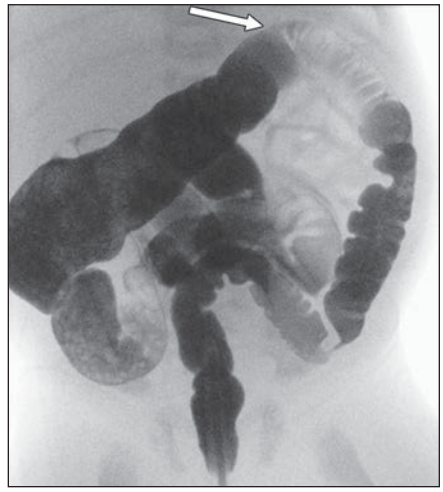

Fig. 14—2-week-old boy with long-segment Hirschsprung disease. Frontal view from enema with contrast material shows transition point (*arrow*) near splenic flexure. Although this may initially be confused with functional immaturity of colon, rectum is not widest portion of colon, raising suspicion of long segment Hirschsprung disease, which was confirmed with biopsy.

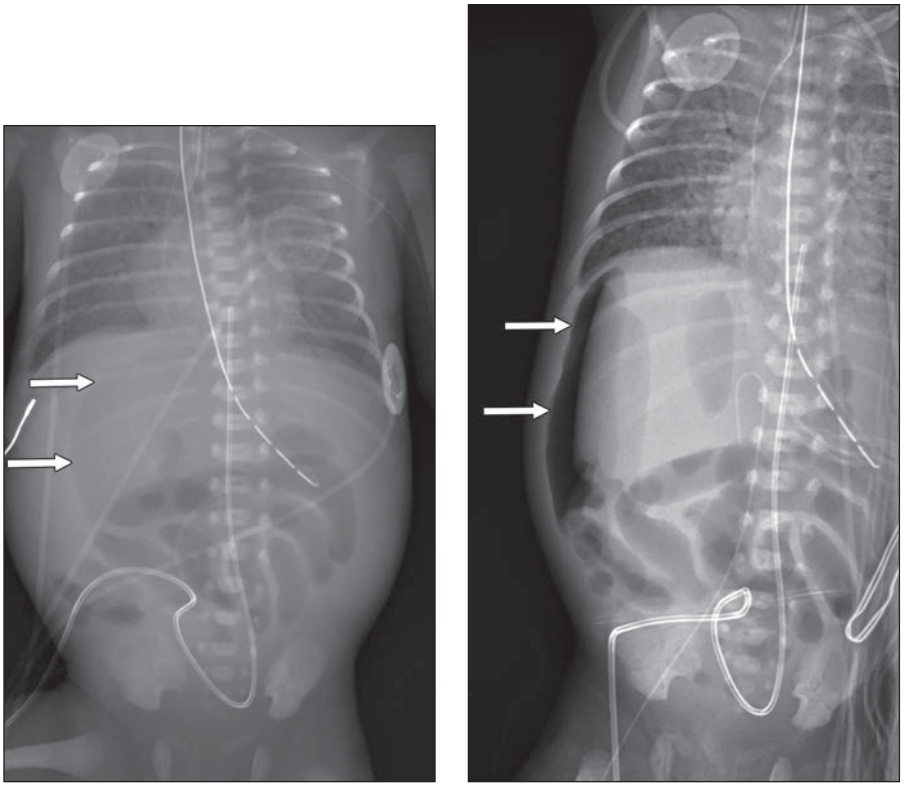

Fig. 15—9-day-old 24-week-premature girl with necrotizing enterocolitis and pneumoperitoneum. **A** and **B,** Frontal chest and abdomen radiograph (**A**) shows multiple distended stacked bowel loops, with large pneumoperitoneum (*arrows*), which is better seen on left lateral decubitus view (*arrows*, **B**). No definite pneumatosis or portal venous gas were present. Changes of surfactant deficiency disorder are noted in bilateral lungs.

FOR YOUR INFORMATION

This article is available for CME and Self-Assessment (SA-CME) credit that satisfies Part II requirements for maintenance of certification (MOC). To access the examination for this article, follow the prompts associated with the online version of the article.